HHS Public Access

Author manuscript

Genes Chromosomes Cancer. Author manuscript; available in PMC 2018 October 01.

Published in final edited form as:

Genes Chromosomes Cancer. 2017 October ; 56(10): 719–729. doi:10.1002/gcc.22476.

Genomic and metabolic characterization of a chromophobe renal cell carcinoma cell line model (UOK276)

Youfeng Yang[1], **Cathy D. Vocke**[1], **Christopher J. Ricketts**[1], **Darmood Wei**[1], **Hesed M. Padilla-Nash**[2], **Martin Lang**[1], **Carole Sourbier**[1], **J. Keith Killian**[2], **Shawna L. Boyle**[1], **Robert Worrell**[1], **Paul S. Meltzer**[2], **Thomas Ried**[2], **Maria J. Merino**[3], **Adam R. Metwalli**[1], and **W. Marston Linehan**[1]

[1]Urologic Oncology Branch, Center for Cancer Research, National Cancer Institute, National Institutes of Health, Bethesda, MD

[2]Genetics Branch, Center for Cancer Research, National Cancer Institute, National Institutes of Health, Bethesda, MD

[3]Laboratory of Pathology, National Cancer Institute, National Institutes of Health, Bethesda, MD

Abstract

Chromophobe renal cell carcinoma (ChRCC) represents 5% of all RCC cases and frequently demonstrates multiple chromosomal losses and an indolent pattern of local growth, but can demonstrate aggressive features and resistance to treatment in a metastatic setting. Cell line models are an important tool for the investigation of tumor biology and therapeutic drug efficacy. Currently, there are few ChRCC-derived cell lines and none is well characterized. This study characterizes a novel ChRCC-derived cell line model, UOK276. A large ChRCC tumor with regions of sarcomatoid differentiation was used to establish a spontaneously immortal cell line, UOK276. UOK276 was evaluated for chromosomal, mutational and metabolic aberrations. The UOK276 cell line is hyper-diploid with a modal number of 49 chromosomes per cell, and evidence of copy-neutral loss of heterozygosity, as opposed to the classic pattern of ChRCC chromosomal losses. UOK276 demonstrated a *TP53* missense mutation, expressed mutant TP53 protein, and responded to treatment with a small molecule therapeutic agent, NSC319726, designed to reactivate mutated TP53. Xenograft tumors grew in nude mice and provide an *in vivo* animal model for the investigation of potential therapeutic regimes. The xenograft pathology and genetic analysis suggested UOK276 was derived from the sarcomatoid region of the original tumor. In summary, UOK276 represents a novel *in vitro* and *in vivo* cell line model for aggressive, sarcomatoid-differentiated, *TP53* mutant ChRCC. This pre-clinical model system could be used to investigate the novel biology of aggressive, sarcomatoid ChRCC and evaluate new therapeutic regimes.

Correspondence W. Marston Linehan, M.D., Urologic Oncology Branch, National Cancer Institute, Building 10 CRC Room 1-5940, Bethesda, MD 20892-1107 USA, Tel: 301-496-6353, Fax: 301-402-0922, WML@nih.gov.

The authors declare that no competing interests exist.

INTRODUCTION

It is now widely accepted that renal cell carcinoma (RCC) is not a single entity, but consists of a heterogeneous group of cancers that all arise from within the kidney and can be subtyped by histopathological features.[1,2] While clear cell and papillary renal cell carcinoma represent the most common subtypes of renal cell carcinoma (~75% and ~15% of cases respectively), chromophobe renal cell carcinoma (ChRCC) represents a rarer tumor subtype accounting for ~5% of kidney tumors resulting in 3,000 new cases per year in the United States.[3–5]

ChRCC can present as a component of a cancer predisposition syndrome and is associated with germline mutation of *FLCN* in Birt-Hogg-Dubé (BHD) syndrome and with germline mutation of *PTEN* in Cowden syndrome.[6–9] Sporadic ChRCC is associated with mutation of the *TP53* and *PTEN* genes and typically demonstrates a well established karyotype of multiple chromosomal losses with loss of one complete copy of chromosomes 1, 2, 6, 10, 13, and 17.[10,11] Although ChRCC typically exhibits an indolent pattern of local growth, with greater than 90% ten-year cancer-specific survival, aggressive features and metastasis can occur and demonstrate resistance to treatment in a metastatic setting.[12,13] Some ChRCC's demonstrate regions of sarcomatoid differentiation (~2%) which is associated with more aggressive disease and poorer patient outcome.[13,14]

Due to its relative rarity, ChRCC is less well studied than other RCC subtypes. Cell line models are an important tool for both the investigation of tumor biology and therapeutic drug efficiency. Currently, numerous cell line models exist that have been derived from patients with clear cell or papillary RCC; however, there are few cell lines derived from ChRCCs and none that is well characterized and commonly used.[15,16] In the present report we describe the initial characterization of the genetic and metabolic profile of a novel ChRCC-derived cell line model.

MATERIALS AND METHODS

Patient

The patient was evaluated and managed at the Hatfield Clinical Research Center, National Institutes of Health (NIH). Peripheral blood and tumor samples were obtained for DNA extraction. This study was approved by the Institutional Review Board of the National Cancer Institute and the patient provided written informed consent.

Cell line production protocol

The UOK276 cell line was established from a section of tumor tissue removed at surgery following the protocols and techniques previously described by the Urologic Oncology Branch.[17] The UOK276 cells were propagated for over 20 passages with a passage being performed every 2–3 days by splitting 1 to 2. The immortalized normal kidney cell line HK-2 and the normal human primary renal proximal tubule epithelial cells PSC-400 were purchased from the American Type Culture Collection (ATCC) and the normal human renal cortical epithelial cells HRCE were purchased from Lonza (Lonza Inc., NJ). All cells were

cultivated in DMEM medium containing 25mM D-glucose and supplemented with 10% fetal calf serum and 2 mM L-glutamine.

Mouse xenograft protocol

Approximately 1×10^6 UOK276 cells were suspended in a 0.2 ml mixture of 50% PBS and 50% Matrigel® Matrix (Corning Life Sciences, MA) and subcutaneously injected into 10 athymic nude mice to evaluate the tumorigenic potential of this cell line. All animal care protocols used had been approved by the Institutional Animal Care and Use Committee (IACUC) and were in accordance with National Cancer Institute guidelines.

RNA extraction and Real-Time PCR analysis

Total RNA was extracted from cell lines grown in 10 cm dishes using Trizol Reagent (Invitrogen, CA) and following the standard protocol. Cell lines were grown to a confluency of approximately 80–90%, washed with 5 ml of sterile PBS and lysed using 1 ml of Trizol Reagent. Following the standard RNA extraction protocol, the RNA was re-suspended in 50 μl of RNase-Free water and the RNA concentration was measured using a NanoDrop 2000 UV-Vis Spectrophotometer (Thermo Fisher Scientific Inc., MA). For each cell line, cDNA was synthesized from 2 μg of total mRNA using the SuperScript® VILO™ cDNA Synthesis Kit (Invitrogen) in a 20 μl volume. The cDNAs were diluted 10-fold with 180 μl of RNase-Free Water and 2 μl was used in 10 μl reaction volume for RT-PCR amplification using an ABI ViiA7 real-time PCR system (Thermo Fisher Scientific Inc.). Expression levels were normalized to the control *ACTB* housekeeping gene (Hs99999903_m1) and calculated using the ViiA7 software as comparative CT (ΔΔCT) values. The non-immortalized normal kidney cell line HRCE was designated to represent the normal expression level with a value of 1. TaqMan® Gene Expression Assays (Thermo Fisher Scientific Inc.) were used to assess the expression levels of several genes within the electron transport chain complexes, *NDUFA3* (Hs01547166_m1), *NDUFA6* (Hs00899690_m1), *UQCRB* (Hs00559884_m1), *COX5A* (Hs00362067_m1), *COX6C* (Hs00269977_m1), *ATP5B* (Hs00969569_m1), and the *MYC* gene (Hs00153408_m1).

Metabolic flux analysis protocol

An XF96 Extracellular Flux Analyzer (Seahorse Bioscience, MA) was used to evaluate the basal level of cellular respiration in the UOK276 cells in comparison to an immortalized normal kidney cell line HK-2 and two non-immortalized normal kidney epithelial cell lines (HRCE and PSC-400). All cell lines were cultured in custom XF96 microplates and the cells were seeded at a starting concentration of 10,000 cells/well 24 h before being measured. Immediately before measurements were taken, fresh medium was added and the basal levels of O_2 consumption were measured for 90 min. All cell lines were measured in a single experiment with 6 replicates for each cell line.

Spectral karyotyping (SKY) and MYC gene locus analysis

SKY was performed on 25 UOK276 metaphase spreads and were scored for chromosomal copy number and for structural aberrations as previously described.[18] Spectrum-based classification and analysis of the fluorescent images was performed by using SkyView

software (Applied Spectral Imaging [ASI], CA). The chromosome complements of every metaphase spread were analyzed and the karyotypes were described according to human chromosome nomenclature standards described in ISCN 2009.[19] Structural aberrations and numerical chromosomal gains were considered clonal if two or more cells contained the same change, while numerical chromosomal losses were considered clonal if three or more cells demonstrated the same loss.[18,19] Fluorescence *in situ* hybridization (FISH) was performed on the *MYC* gene locus using the Vysis LSI MYC dual color break apart rearrangement probe set (Abbott Laboratories, IL) according to manufacturer's instructions. This evaluated the copy number for this locus and assessed whether chromosome translocation had separated the *MYC* promoter from the *MYC* gene.

DNA Sanger sequencing

DNA was extracted from cell pellets using a Promega Maxwell 16 Cell DNA Purification Kit or from FFPE unstained slides from chromophobe and sarcomatoid tumor areas using a Maxwell 16 FFPE Tissue LEV DNA Purification Kit (Promega, WI, USA). The UOK276 cell line DNA was assessed using the OncoVar assay in collaboration with the Genetics Branch at NCI. The OncoVar v3 assay tests a sample by hybrid capture sequencing analysis for genomic variants within a panel of 240 cancer-related genes, including the known kidney cancer pathogenicity genes.[20,21] Mutations in *TP53*, *TRAF7*, *SMARCA4*, and *SMO* were validated by PCR using a Qiagen Taq PCR Core Kit (Qiagen, MD) according to the manufacturer's specifications, followed by bidirectional sequencing using the BigDye Terminator v.1.1 Cycle Sequencing Kit (Applied Biosystems, CA,) according to the manufacturer's specifications. Sequence reactions were cleaned with Performa DTR Plates (Edge Bio, MD) and capillary electrophoresis was performed on an ABI 3730/ABI 3130xl Genetic Analyzer automated sequencing machine (Applied Biosystems). Forward and reverse sequences were evaluated using Sequencher 5.4.6 (Genecodes, MI). Primers used were TP53-For: CAGTTGCTTTATCTGTTCACTTG, TP53-Rev: CACTGACAACCACCCTTAAC, TRAF7-For: CTGGGCTCCATCTCTCAAG, TRAF7-Rev: TCTGCAGGCAACACCAGATC, SMARCA4-For: CGCAGAGTGGGAGATTCTC, SMARCA4-Rev: ACCTGGAACCGTCAGCATG, SMO-For: GTTCCAAAGTTTGCGAAGTTG, SMO-Rev: AGCCCAGGCACACGTTGTAG.

Mitochondrial (mt)DNA sequencing

The entire mitochondrial genome was sequenced and analyzed as previously described.[22] In brief, the entire mitochondrial genome was amplified from whole genomic DNA as overlapping PCR fragments using KAPA2G Fast Readymix (KAPA Biosystems, MA) and sequenced with BigDye Terminator v.1.1 Cycle Sequencing Kit (Applied Biosystems). Sequence reactions were cleaned with Performa DTR Plates (Edge Bio) and capillary electrophoresis was performed on an ABI 3730/ABI 3130xl Genetic Analyzer automated sequencing machine (Applied Biosystems). Sequences were aligned to the human mitochondrial reference sequence (NC_012920) using Sequencher 5.4.6 (Genecodes, MI).

Western blotting

Sub-confluent cells were trypsinized and washed once in PBS. Total proteins were extracted by solubilizing the cell pellets in urea buffer (8 M urea, 0.1 M NaH2PO4, 10 mM Tris pH 8,

0.1% mercaptoethanol). Protein concentration was quantified by the Bio-Rad protein assay (Bio-Rad Laboratories, CA). Proteins (30 μg) were separated by electrophoresis on NuPage™ 4% to 20% Bis-Tris gels (Life Technologies Corporation, CA) and transferred onto Immobilon-P membranes (Millipore, MA) according to the manufacturers' directions. Western blot analyses of proteins were carried out by using anti-Ku80 (C48E7) (Cell Signaling Technology Inc., MA) and anti-p53 clone DO-7 (Dako North America, CA) antibodies. The primary antibodies were detected using fluorescently labeled anti-mouse and anti-rabbit secondary antibodies at a dilution of 1:10,000 and obtained from Li-Cor and were visualized by scanning the blots on a Li-Cor Odyssey® (LiCOR, NE).

Drug treatment and growth assay protocol

The cells were seeded onto 96 well plates and treated with the NSC319726 at 0 and 10 nM in triplicate. Cell proliferation was measured by MTT assay (Sigma-Aldrich, MO) every 24 h for 5 days. The MTT assay was conducted according the manufacturer's instructions.

FACS protocol

Cells were incubated with 10 μM BrdU for 2 h prior to harvest. Cells were then trypsinized and fixed overnight at 4°C in 70% ethanol in calcium- and magnesium-free phosphate buffered saline (PBS). Ethanol solution was removed and cells were incubated in 3 ml of 0.08% pepsin in 0.1 N HCl at 37°C for 20 min. Pepsin was removed and nuclei were incubated in 1.5 ml of 2 N HCl at 37°C for 20 min. The nuclei containing acid solution was neutralized with 3 ml of 0.1 M sodium borate. Nuclei were spun out of neutralized acid and washed with 2 ml IFA buffer (10 mM HEPES pH 7.4, 150 mM NaCl, 4% FBS and 0.1% sodium azide with 0.5% Tween-20 added on the day of use) and then incubated overnight at 4°C with anti-BrdU clone MoBU-1 conjugated to AlexaFluor488 (Invitrogen B35130) in IFA buffer. DNA was stained for 30 min with IFA buffer with of 50 μg/ml propidium iodide (PI) (Sigma-Aldrich P4864) and 5 μg/ml RNase A (Sigma R4642). Cell cycle analysis (bivariate plots of BrdU incorporation and DNA content) was performed on a FACSCanto II (Becton Dickinson, NJ). Data were collected and analyzed using FlowJo software (FlowJo, OR).

Invasion assay

Invasion assays were performed using the RT-CIM™ system (Acea Biosciences, CA) as previously described.[23] In brief, UOK276 cells were cultured overnight in serum-free media, plated in triplicate at a density of 40,000 cells per well and treated with either 1nM NSC319726, 10nM NSC319726 or DMSO at the beginning of the experiment. Invasion assays were performed at 37°C and 5% CO_2 and data was recorded in real time for a minimum of 90 h.

RESULTS

Derivation of the UOK276 cell line from a sporadic chromophobe RCC

A 45-year-old male patient presented with a history of a large left renal lesion that had been incidentally identified due to an evaluation for an umbilical hernia. Contrast MRI imaging identified a 16 cm solid mass arising from the midportion of the left kidney (Figure 1A, 1B).

In addition, a 2.4 cm by 1.4 cm hypoenhancing left para-aortic mass was observed, potentially indicating metastatic disease, and multiple T2 hyperintensities were identified within the right kidney, the larger of which were compatible with simple cysts (Figure 1A). A radical nephrectomy with lymph node dissection was performed. The 20 cm by 15.5 cm by 12 cm renal tumor was found to have replaced the majority of the normal kidney and the histopathologic evaluation identified it as a chromophobe (Ch)RCC (Figure 1C) with regions of sarcomatoid differentiation (Figure 1D). Metastatic renal cell carcinoma was found in 2 out of 40 periaortic lymph nodes and in 1 out of ten hilar lymph nodes. Procured tissue from the primary renal tumor was used to derive a new, spontaneously immortal cell line, UOK276, which was passaged over 20 times and successfully cryogenically frozen and subsequently revived.

Approximately 5 million UOK276 cells were injected into the flank of 10 athymic nude mice. This produced measurable xenograft tumors in all injected mice. The xenograft tumors grew relatively rapidly with 1cm diameter tumors being observed approximately 50 days after injection (Figure 1E). Notably, the xenograft tumors did not demonstrate the classic chromophobe histology, but resembled the higher grade, sarcomatoid regions of the original tumor (Figure 1E).

Metabolic analysis of the UOK276 cell line

The recent TCGA study of ChRCC demonstrated increased expression of several electron transport chain (ETC) genes in chromophobe tumors compared to the surrounding normal kidney tissue, suggesting increased usage of oxidative phosphorylation within these tumors.[24] Messenger RNA expression analysis was performed on 6 genes (*NDUFA3*, *NDUFA6*, *UQCRB*, *COX5A*, *COX6C* and *ATP5B*) representing electron transport chain complexes I, III, IV and V that had been previously shown to be up-regulated in ChRCC. UOK276 demonstrated either normal or reduced levels of mRNA expression in these selected ETC-related genes in comparison to a non-immortalized normal kidney cell line, HRCE (Figure 2A). For several genes UOK276 demonstrated the same level of down-regulation observed within a clear cell RCC derived cell line UOK139, which reflects the decreased usage of oxidative phosphorylation reported in sporadic clear cell RCC (Figure 2B).[25] This was supported by an assessment of live cells using a Seahorse flux analyzer that demonstrated a relatively low level of oxygen consumption (OCR) in UOK276 in comparison to an immortalized normal kidney cell line, HK-2, and two non-immortalized normal kidney epithelial cell lines, HRCE and PSC-400 (Figure 2B).

Chromosomal copy number analysis of the UOK276 cell line

Most ChRCCs demonstrate a classic pattern of chromosomal losses that includes single losses of chromosomes 1, 2, 6, 10, 13 and 17. In the UOK276 cell line, the SKY analysis demonstrated that the majority of cells were hyper-diploid with a modal number of 49 chromosomes per cell and a chromosome number range of 43–99. SKY analysis revealed clonal losses of chromosomes 1, 3, 4, 11, 13, 14, and 19 and clonal gains of the X and Y chromomes and chromosomes 6, 8, and 20. In addition, SKY analysis identified two balanced translocations between chromosomes 8 and X, t(X;8)(q26;q24), and chromosomes18 and 22, t(18;22)(p11.2;q11.2) (Figure 3A). The break on 8q occurred near

the *MYC* gene locus, but break-apart FISH analysis demonstrated no alterations to *MYC* and no significant increase in *MYC* mRNA expression was demonstrated, although amplification of this derivative chromosome was observed (Supporting Information Figure 1).

This variation from the classic pattern of chromosomal losses in ChRCC may be due to the cell line being derived from the portion of the tumor that had undergone sarcomatoid differentiation. It was noticeable that the chromosomal pattern contained two copies of the reciprocal translocations involving chromosomes 18 and 22, but no normal copies of chromosomes 18 or 22 (Figure 3A). Additionally, cells demonstrated two Y chromosomes and two copies of the reciprocal translocations involving chromosomes 8 and X, although a normal copy of chromosome 8 was also present (Figure 3A). This observation suggests that a chromosome doubling event may have occurred within the UOK276 cell line resulting in multiple copies of only one of the chromosomes present within the original cells. Supporting this hypothesis was the observation that upon performing STR analysis on the UOK276 cell line 14 out of the 15 highly variable markers evaluated were homozygous with only the marker on chromosome 8 demonstrating heterozygosity in line with the presence of both derivative and wild-type chromosome 8s (Figure 3B and Supporting Information Figure 2). In contrast, the STR analysis of the patient's blood DNA demonstrated informative variation in 11 out of 15 markers on chromosomes 4, 5, 8, 11, 12, 15, 16, 18, and 21 that all showed loss of heterozygosity in UOK276 except the marker on chromosome 8 (Figure 3B).

Mutational analysis of the UOK276 cell line

DNA from the UOK276 cell line was evaluated using the OncoVar v3 assay, an oncogene panel sequencing analysis that tests a sample by hybrid capture sequencing for genomic variants in 240 cancer-related genes, including the known kidney cancer pathogenicity genes. In addition, DNA was extracted from both the classic-chromophobe and sarcomatoid regions of the original tumor and from the blood of the patient in order to provide the germline mutational status using Sanger sequencing. A heterozygous missense mutation (p.H193Y) of the *TP53* gene, the most commonly mutated gene in sporadic ChRCC,[24] was present in the sarcomatoid tumor region and was homozygously mutated in UOK276 (Figure 4A). This mutation was not detected in the classic-chromophobe tumor region or in the germline blood DNA (Figure 4A). A deletion/insertion event that resulted in an in-frame loss of 4 amino acids (del T22-P25) was identified in the *TRAF7* gene that was homozygously mutated in UOK276 and in the sarcomatoid tumor region and heterozygously mutated in the classic-chromophobe tumor region and in the germline blood DNA (Figure 4B). A small number of mutations within the *TRAF7* gene have been previously identified within sporadic cases of clear cell, papillary and chromophobe renal cell carcinomas (Figure 4B). Two further mutations were identified: a missense mutation of *SMARCA4* (p.T910M) and an in-frame insertion of a leucine residue in *SMO* (p.G16GL), and both were present homozygously in UOK276 and not detected in the germline blood. In combination with the copy number and STR analysis results, this is likely to represent copy-neutral loss of heterozygosity.

The TCGA study of ChRCC identified several non-synonymous mutations in the electron transport genes encoded within the mitochondrial genome that associated with eosinophilic ChRCC. Evaluation of both the primary tumor and the UOK276 cell line demonstrated no novel or pathogenic alterations to the mitochondrial genome and identified the patient as having the H40a haplogroup consistent with a European ancestry.

Functional and therapeutic investigation of the *TP53* mutation

Somatic gain of the p.H193Y *TP53* missense mutation has been previously associated with multiple different cancer types and is considered a pathogenic recurrent hotspot mutation.[26] Protein expression analysis demonstrated the presence of the mutant TP53 protein in the UOK276 cell line with signal for the wild-type protein in the HK-2 normal kidney cell line (Figure 5A). A small molecule therapeutic agent, NSC319726, originally designed to reactivate mutated TP53 with the nearby p.R175H/L missense mutations, has been shown to be effective in reactivating other missense mutations.[27,28] A single dose of 10 nM NSC319726 resulted in an approximately 70% reduction in the growth of UOK276 over 5 days although a lesser effect was also observed in the HK-2 normal kidney cell line (Figure 5B). Additionally, real-time cell invasion analysis performed over a 90-hour period demonstrated a dose dependent suppression of invasion in UOK276 cells in response to a single starting dose of either 1 nM or 10 nM NSC319726 (Figure 5C). Importantly, reactivation of TP53 should result in disruption of the cell cycle and FACS analysis comparing increasing doses of NSC319726 demonstrated a significantly greater and dose-dependent inhibition of the cell cycle in UOK276 cells in comparison to the HK-2 cells (Figure 5D).

DISCUSSION

Chromophobe renal cell carcinoma represents a rare and understudied subtype of RCC. The establishment of cell line models for any given cancer can be extremely useful and allow for numerous biological and therapeutic investigations that would be very challenging to perform with less relevant models. This study describes a novel cell line model, UOK276, derived from an aggressive chromophobe renal cell carcinoma with regions of sarcomatoid differentiation. UOK276 grows rapidly in tissue culture as an *in vitro* model and produces xenograft tumors in nude mice as an *in vivo* model. Both these models could be used to investigate the biology of aggressive ChRCC with sarcomatoid differentiation and evaluate new therapeutic approaches.

A small number of ChRCC cell line models have been previously published but none has been widely utilized or extensively characterized.[15,16] In Gerharz *et al.*[15], two cell lines were derived from the same chromophobe RCC tumor and both demonstrated the classic pattern of chromosomal loss and neither was assessed for somatic mutations. In Valente *et al.*[16], two cell lines were derived from two different chromophobe RCC tumors to demonstrate a novel method of cell line production, but genetic analysis was not performed on those cell lines.

It is important that cell line models accurately represent the histologic tumor type being studied. ChRCCs represents ~5% of all cases of RCC[3–5] and typically present with an indolent pattern of local growth that is most often amenable to surgical resection.[12,13] A

review of published literature by Amin *et al.*[29] reported the 5-year and 10-year survival rates for ChRCC ranging from 78% to 100% and 80% to 90% respectively. However, ChRCC tumors have been shown to demonstrate sarcomatoid differentiation at a relatively high frequency. Most studies identified sarcomatoid differentiation in 8–9% of ChRCCs, including 5 of 53 (9.4%) tumors in de Peralta-Venturina *et al.*[30], 9 of 103 (8.7%) tumors in Cheville *et al.*[31], and 12 of 145 (8.3%) tumors in Amin *et al.*[29], while Przybycin *et al.*[13] only observed sarcomatoid differentiation in 4 of 203 tumors (2.0%). The sarcomatoid differentiation in these more aggressive ChRCCs has been shown to associate with higher rates of metastasis and significantly poorer patient prognosis.[29,31] Therefore, a model for those aggressive ChRCC tumors would provide a useful platform for testing novel therapeutic agents. UOK276 represents an example of these more aggressive tumors as it was created from material provided by a patient that presented with a large tumor with sarcomatoid differentiation, an early age of onset, and metastatic disease. Importantly, the UOK276 cell line appears to be derived from the sarcomatoid region of the original tumor with both the pattern of mutations and histopathological presentation within the xenograft tumors being consistent with this origin. The UOK276 cell line does not show the classic pattern of chromosomal losses commonly observed within the majority of ChRCCs[10,11], but previously published analyses of ChRCC with sarcomatoid differentiation have also demonstrated this absence of the classic chromosomal loss pattern within sarcomatoid regions.[14,32,33] In Brunelli *et al.*[32], the sarcomatoid transformed regions showed either a normal copy number or an increased copy number for the classically lost chromosomes 1, 2, 6, 10, and 17. In addition, the TCGA study of chromophobe RCC identified three ChRCCs with evidence of sarcomatoid features and two of those tumors demonstrated no chromosomal losses.[24] The chromosomal copy number pattern shown by UOK276 is completely consistent with these previous observations in patient primary tumors. In addition, UOK276 demonstrates evidence for copy-neutral loss of heterozygosity. Specifically, the STR analysis demonstrated a significant loss of variation in informative markers in the tumor compared to the normal blood with no loss of chromosomal number, the mutations identified in UOK276 were all homozygous, and duplicate copies of specific derivative chromosomes were present with no evidence of the wild-type chromosomes. A potential mechanism for this could involve the initial loss of a large number of chromosomes, an event common to ChRCCs, which led to a critically low chromosomal number that resulted in an internal chromosomal duplication and copy-neutral loss of heterozygosity. The metabolic analysis of UOK276 did not demonstrate the expected up-regulation of the oxidative phosphorylation-related genes or associated increase in oxygen consumption [24]. This altered metabolism could be associated with sarcomatoid differentiation and represent a more aggressive phenotype, but this requires further investigation and the analysis of other sarcomatoid ChRCC samples. Thus, UOK276 potentially provides a useful model of sarcomatoid differentiation in an aggressive chromophobe RCC.

Mutation of the *TP53* gene is a relatively common event in chromophobe RCC with 32% of the ChRCCs analyzed by the Cancer Genome Atlas (TCGA) demonstrating somatic mutation of *TP53*.[24] In addition, it has been proposed that the gains of somatic *TP53* mutations are associated with sarcomatoid transformation/differentiation in kidney cancer,

although in ChRCC somatic mutation of *TP53* is far more common than sarcomatoid differentiation.[34,35] The UOK276 cell line demonstrates a known pathogenic recurrent hotspot mutation, p.H193Y, which was only present in the sarcomatoid region of the original tumor.[26] This provides a model of TP53 mutant, sarcomatoid ChRCC that still expresses the mutant TP53 protein for potential therapeutic investigation. Several small molecules have been designed to reactivate missense mutant TP53 protein by restoring the wild-type structure or function, such as NSC319726 (ZMC1).[27,28] NSC319726 was initially demonstrated reactivate the most common TP53 missense mutant (p.R175H) and subsequently shown to reactivate several other TP53 missense mutations (e.g. p.C176F, p.C238S, p.C242S, p.G245S).[27,28] In these mutations, the DNA binding function of the mutant protein had been altered due to incorrect zinc-binding inducing misfolding of the protein and this zinc-binding is subsequently corrected by NSC319726.[28] The p.H193Y TP53 mutation had also been predicted to alter the ability of TP53 to bind to DNA and thus was considered to be potentially targetable.[36] In this study, some interesting initial data suggests that the mutant TP53 protein had regained some functionality as treatment with NSC319726 inhibited both proliferation and invasion and resulted in significant alteration and inhibition of the cell cycle. Further investigation of the effects of the NSC319726 small molecule inhibitor on TP53 protein in these cells could provide a new targeted therapeutic option for treating tumors with this hotspot mutation.

In addition to the somatically gained *TP53* mutation, the UOK276 cell line demonstrated a mutation of the tumor necrosis factor receptor-associated factor 7 (*TRAF7*) gene that was present heterozygously in the patient's germline and the chromophobe-like region of the tumor and showed loss of heterozygosity in the sarcomatoid region and in UOK276. *TRAF7* encodes an E3 ubiquitin ligase that potentiates MEKK3 signaling and promotes apoptosis.[37] Recently, mutations in *TRAF7* have been associated with non-NF2 mutant meningioma, a largely benign form of brain tumor.[38] The complete relevance of this mutation has yet to be elucidated but the patient presented with a large 16 cm tumor at only 45 years of age and this could be suggestive of a germline genetic component to his disease.[39].

In summary, the UOK276 cell line represents a novel *in vitro* and *in vivo* model for aggressive, sarcomatoid-differentiated, TP53 mutant chromophobe renal cell carcinoma. This pre-clinical model system could be useful for investigation of the novel biology of aggressive, sarcomatoid ChRCC as well as to evaluate new therapeutic approaches for patients with advanced ChRCC, such as those that target mutant TP53.

Supplementary Material

Refer to Web version on PubMed Central for supplementary material.

Acknowledgments

This research was supported by grants provided by the Intramural Research Program of the NIH, National Cancer Institute, Center for Cancer Research (ZIA BC011028, ZIA BC011038, ZIA BC011089, and ZIC BC011044). The content of this publication does not necessarily reflect the views or policies of the Department of Health and Human Services nor does mention the trade names, commercial products or organizations imply endorsement by the U.S. Government.

References

1. Linehan WM, Srinivasan R, Schmidt LS. The genetic basis of kidney cancer: a metabolic disease. Nature Reviews Urology. 2010; 7(5):277–285. [PubMed: 20448661]
2. Linehan WM. Genetic basis of kidney cancer: role of genomics for the development of disease-based therapeutics. Genome Res. 2012 genome.cship.org 10-15-2012.
3. Storkel S, Eble JN, Adlakha K, et al. Classification of renal cell carcinoma: Workgroup No. 1. Union Internationale Contre le Cancer (UICC) and the American Joint Committee on Cancer (AJCC). Cancer. 1997; 80(5):987–989. [PubMed: 9307203]
4. Peyromaure M, Misrai V, Thiounn N, et al. Chromophobe renal cell carcinoma: analysis of 61 cases. Cancer. 2004; 100(7):1406–1410. [PubMed: 15042674]
5. Chow WH, Dong LM, Devesa SS. Epidemiology and risk factors for kidney cancer. Nat Rev Urol. 2010; 7(5):245–257. [PubMed: 20448658]
6. Nickerson ML, Warren MB, Toro JR, et al. Mutations in a novel gene lead to kidney tumors, lung wall defects, and benign tumors of the hair follicle in patients with the Birt-Hogg-Dube syndrome. Cancer Cell. 2002; 2(2):157–164. [PubMed: 12204536]
7. Pavlovich CP, Walther MM, Eyler RA, et al. Renal tumors in the Birt-Hogg-Dub, syndrome. Am J Surg Pathol. 2002; 26(12):1542–1552. [PubMed: 12459621]
8. Schmidt LS, Warren MB, Nickerson ML, et al. Birt-Hogg-Dube syndrome, a genodermatosis associated with spontaneous pneumothorax and kidney neoplasia, maps to chromosome 17p11.2. American Journal of Human Genetics. 2001; 69(4):876–882. [PubMed: 11533913]
9. Shuch B, Ricketts CJ, Vocke CD, et al. Germline PTEN mutation Cowden syndrome: an underappreciated form of hereditary kidney cancer. J Urol. 2013; 190(6):1990–1998. [PubMed: 23764071]
10. Speicher MR, Schoell B, du Manoir S, et al. Specific loss of chrmosoomes 1,2,6,10,13,17, and 21 in chromophobe renal cell carcinomas revealed by comparative genomic hybridization. American Journal of Pathology. 1994; 145:356–364. [PubMed: 7519827]
11. Brunelli M, Eble JN, Zhang S, Martignoni G, Delahunt B, Cheng L. Eosinophilic and classic chromophobe renal cell carcinomas have similar frequent losses of multiple chromosomes from among chromosomes 1, 2, 6, 10, and 17, and this pattern of genetic abnormality is not present in renal oncocytoma. Mod Pathol. 2005; 18(2):161–169. [PubMed: 15467713]
12. Amin MB, Tamboli P, Javidan J, et al. Prognostic impact of histologic subtyping of adult renal epithelial neoplasms: an experience of 405 cases. Am J Surg Pathol. 2002; 26(3):281–291. [PubMed: 11859199]
13. Przybycin CG, Cronin AM, Darvishian F, et al. Chromophobe renal cell carcinoma: a clinicopathologic study of 203 tumors in 200 patients with primary resection at a single institution. Am J Surg Pathol. 2011; 35(7):962–970. [PubMed: 21602658]
14. Kuroda N, Tamura M, Hes O, Michal M, Gatalica Z. Chromophobe renal cell carcinoma with neuroendocrine differentiation and sarcomatoid change. Pathol Int. 2011; 61(9):552–554. [PubMed: 21884307]
15. Gerharz CD, Moll R, Storkel S, et al. Establishment and characterization of two divergent cell lines derived from a human chromophobe renal cell carcinoma. Am J Pathol. 1995; 146(4):953–962. [PubMed: 7717462]
16. Valente MJ, Henrique R, Costa VL, et al. A rapid and simple procedure for the establishment of human normal and cancer renal primary cell cultures from surgical specimens. PLoS One. 2011; 6(5):e19337. [PubMed: 21573239]
17. Yang Y, Padilla-Nash HM, Vira MA, et al. The UOK 257 cell line: a novel model for studies of the human Birt-Hogg-Dube gene pathway. Cancer Genetics and Cytogenetics. 2008; 180(2):100–109. [PubMed: 18206534]
18. Padilla-Nash HM, Barenboim-Stapleton L, Difilippantonio MJ, Ried T. Spectral karyotyping analysis of human and mouse chromosomes. Nat Protoc. 2006; 1(6):3129–3142. [PubMed: 17406576]
19. Simons A, Shaffer LG, Hastings RJ. Cytogenetic Nomenclature: Changes in the ISCN 2013 Compared to the 2009 Edition. Cytogenet Genome Res. 2013; 141(1):1–6. [PubMed: 23817294]

20. Sorber R, Teper Y, Abisoye-Ogunniyan A, et al. Whole Genome Sequencing of Newly Established Pancreatic Cancer Lines Identifies Novel Somatic Mutation (c.2587G>A) in Axon Guidance Receptor Plexin A1 as Enhancer of Proliferation and Invasion. PLoS One. 2016; 11(3):e0149833. [PubMed: 26962861]
21. Killian JK, Miettinen M, Walker RL, et al. Recurrent epimutation of SDHC in gastrointestinal stromal tumors. Sci Transl Med. 2014; 6(268):268ra177.
22. Lang M, Vocke CD, Merino MJ, Schmidt LS, Linehan WM. Mitochondrial DNA mutations distinguish bilateral multifocal renal oncocytomas from familial Birt-Hogg-Dube tumors. Mod Pathol. 2015; 28(11):1458–1469. [PubMed: 26428318]
23. Tong WH, Sourbier C, Kovtunovych G, et al. The glycolytic shift in fumarate-hydratase-deficient kidney cancer lowers AMPK levels, increases anabolic propensities and lowers cellular iron levels. Cancer Cell. 2011; 20(3):315–327. [PubMed: 21907923]
24. Davis CF, Ricketts CJ, Wang M, et al. The somatic genomic landscape of chromophobe renal cell carcinoma. Cancer Cell. 2014; 26(3):319–330. [PubMed: 25155756]
25. Cancer Genome Atlas Research N. Comprehensive molecular characterization of clear cell renal cell carcinoma. Nature. 2013; 499(7456):43–49. [PubMed: 23792563]
26. Chang MT, Asthana S, Gao SP, et al. Identifying recurrent mutations in cancer reveals widespread lineage diversity and mutational specificity. Nat Biotechnol. 2016; 34(2):155–163. [PubMed: 26619011]
27. Yu X, Vazquez A, Levine AJ, Carpizo DR. Allele-specific p53 mutant reactivation. Cancer Cell. 2012; 21(5):614–625. [PubMed: 22624712]
28. Yu X, Blanden AR, Narayanan S, et al. Small molecule restoration of wildtype structure and function of mutant p53 using a novel zinc-metallochaperone based mechanism. Oncotarget. 2014; 5(19):8879–8892. [PubMed: 25294809]
29. Amin MB, Paner GP, Alvarado-Cabrero I, et al. Chromophobe renal cell carcinoma: histomorphologic characteristics and evaluation of conventional pathologic prognostic parameters in 145 cases. Am J Surg Pathol. 2008; 32(12):1822–1834. [PubMed: 18813125]
30. de Peralta-Venturina M, Moch H, Amin M, et al. Sarcomatoid differentiation in renal cell carcinoma: a study of 101 cases. Am J Surg Pathol. 2001; 25(3):275–284. [PubMed: 11224597]
31. Cheville JC, Lohse CM, Zincke H, et al. Sarcomatoid renal cell carcinoma: an examination of underlying histologic subtype and an analysis of associations with patient outcome. Am J Surg Pathol. 2004; 28(4):435–441. [PubMed: 15087662]
32. Brunelli M, Gobbo S, Cossu-Rocca P, et al. Chromosomal gains in the sarcomatoid transformation of chromophobe renal cell carcinoma. Mod Pathol. 2007; 20(3):303–309. [PubMed: 17277768]
33. Akhtar M, Tulbah A, Kardar AH, Ali MA. Sarcomatoid renal cell carcinoma: the chromophobe connection. Am J Surg Pathol. 1997; 21(10):1188–1195. [PubMed: 9331291]
34. Shuch B, Bratslavsky G, Linehan WM, Srinivasan R. Sarcomatoid renal cell carcinoma: a comprehensive review of the biology and current treatment strategies. The Oncologist. 2012; 17(1):46–54. [PubMed: 22234634]
35. Oda H, Nakatsuru Y, Ishikawa T. Mutations of the p53 gene and p53 protein overexpression are associated with sarcomatoid transformation in renal cell carcinomas. Cancer Res. 1995; 55(3): 658–662. [PubMed: 7834636]
36. Ahn J, Poyurovsky MV, Baptiste N, et al. Dissection of the sequence-specific DNA binding and exonuclease activities reveals a superactive yet apoptotically impaired mutant p53 protein. Cell Cycle. 2009; 8(10):1603–1615. [PubMed: 19462533]
37. Xu LG, Li LY, Shu HB. TRAF7 potentiates MEKK3-induced AP1 and CHOP activation and induces apoptosis. J Biol Chem. 2004; 279(17):17278–17282. [PubMed: 15001576]
38. Clark VE, Erson-Omay EZ, Serin A, et al. Genomic analysis of non-NF2 meningiomas reveals mutations in TRAF7, KLF4, AKT1, and SMO. Science. 2013; 339(6123):1077–1080. [PubMed: 23348505]
39. Shuch B, Vourganti S, Ricketts CJ, et al. Defining Early-Onset Kidney Cancer: Implications for Germline and Somatic Mutation Testing and Clinical Management. J Clin Oncol. 2013

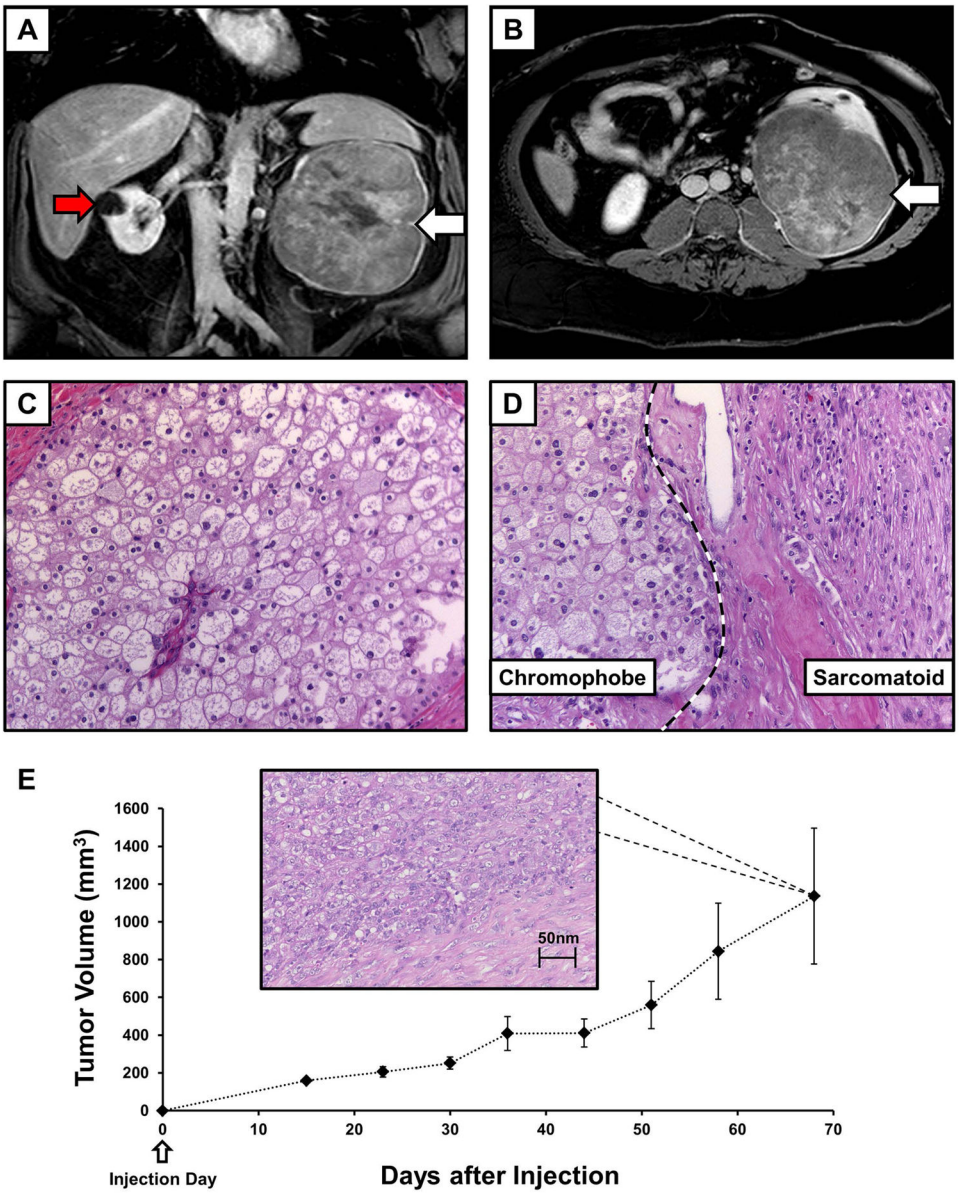

FIGURE 1.

Imaging and histology for the UOK276 cell line. (A) Contrast enhanced MRI T1 coronal imaging demonstrated the size and extent of the tumor in the left kidney (white arrow), as well as a cyst on the right kidney (red arrow). (B) Axial T1 imaging demonstrated that the tumor had almost replaced the entirety of the left kidney (white arrow). (C) Histopathology assessment of an H&E slide demonstrated large polygonal cells with irregular nuclei and well demarcated cellular borders consistent with chromophobe renal cell carcinoma (ChRCC) and (D) identified sarcomatoid areas with the large spindled, pleomorphic cells (original magnification 40x). (E) Ten athymic nude mice were each injected in the flank with ~5 million UOK276 cells resulting in the growth of measurable xenograft tumors in all mice. The xenograft tumors grew rapidly to over 1 cm diameter tumors (>500 mm^3) within approximately 50 days of injection. An example of H & E staining from one of the xenograft

tumors is shown that demonstrates a pathology consistent with the higher grade, sarcomatoid regions of the original chromophobe tumor.

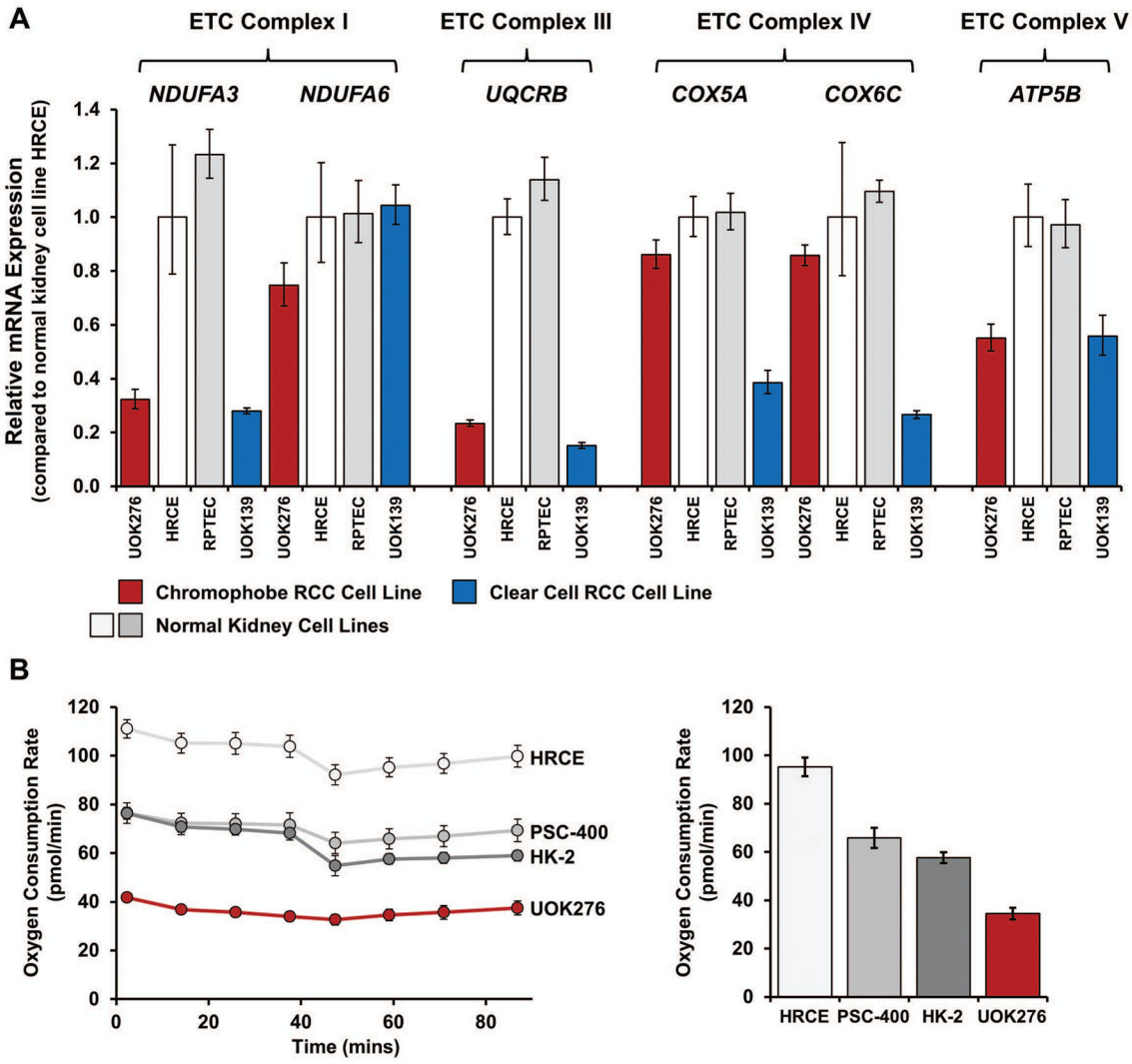

FIGURE 2.

Metabolic analysis of the UOK276 cell line. (A) Most chromophobe RCCs demonstrate increased expression of the genes encoding the components of the electron transport chain (ETC), while clear cell RCCs show decreased expression. TaqMan® mRNA expression analysis for a select number of ETC genes representing ETC complex I (*NDUFA3*, *NDUFA6*), ETC complex III (*UQCRB*), ETC complex IV (*COX5A*, *COX6C*), and ETC complex V (*ATP5B*) was performed to compare the UOK276 cell line with cell lines representing both normal human kidney (HRCE and RPTEC) and clear cell RCC (UOK139). Contrary to expectation, the UOK276 cell line demonstrated lower expression levels of the ETC genes than the normal human kidney cell lines and had an expression pattern that was more similar to the clear cell RCC cell line. (B) The oxygen consumption rate (OCR) for UOK276 was evaluated using a Seahorse XF96 Extracellular Flux Analyzer and compared with three normal kidney control cell lines (HK-2, PSC-400 and HRCE). The OCR was measured for 90 min and a comparison graph at the 60-min time point

demonstrates a lower rate of oxygen consumption in the UOK276 cells that is consistent with the decreased expression of the ETC complex genes.

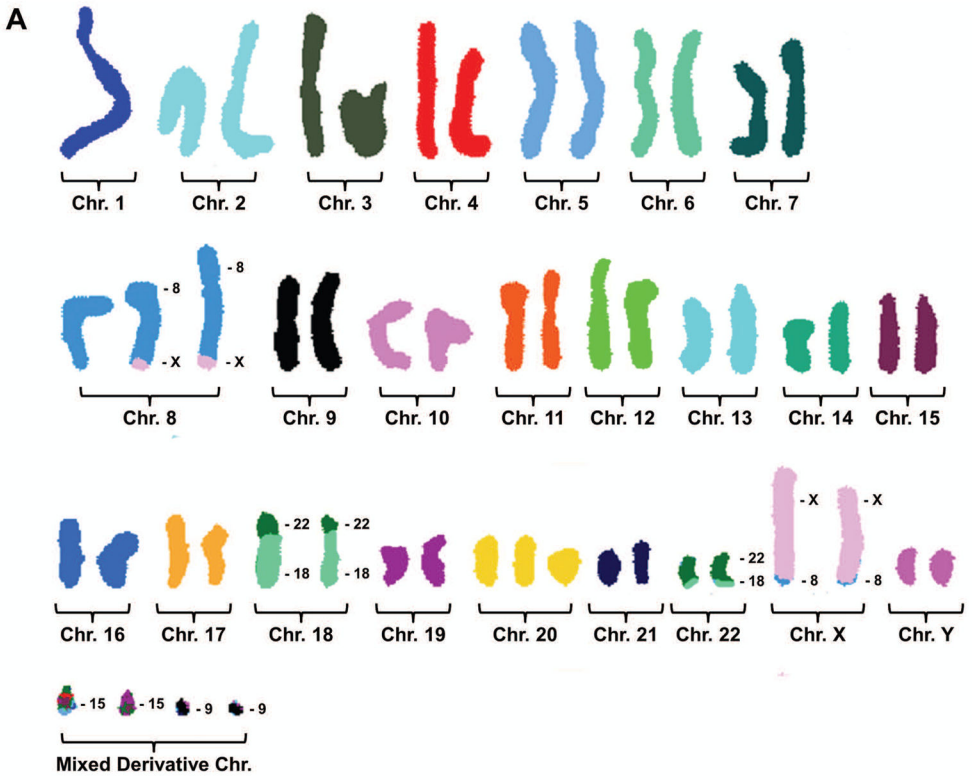

B

	Chr. 2p	Chr. 3p	Chr. 4q	Chr. 5q	Chr. 5q	Chr. 7q	Chr. 8q	Chr. 11p
	TPOX	D3S1358	FGA	D5S818	CSF1PO	D7S820	D8S1179	TH01
UOK276	8	15	20	11	11	11	10, 12	9.3
Blood	8	15	20, 21	11, 12	9, 11	11	10, 12	6, 9.3

	Chr. 12p	Chr. 13q	Chr. 15q	Chr. 16q	Chr. 18q	Chr. 21q	Chr. 21q	Chr. X/Y
	vWA	D13S317	Penta E	D16S539	D18S51	D21S11	Penta D	AMEL
UOK276	16	11	10	10	13	31	10	X, Y
Blood	16, 17	11	10, 16	10, 12	12, 13	30, 31	10, 12	X, Y

FIGURE 3.

Chromosomal analysis of the UOK276 cell line. (A) Spectral karyotyping (SKY) analysis of the UOK276 cell line defined the cells as hyper-diploid, with a modal number of 49 chromosomes per cell, and identified balanced translocations between chromosomes 8 and X, t(X;8)(q26;q24), and chromosomes 18 and 22, t(18;22)(p11.2;q11.2). This does not represent the usual ChRCC hypo-diploid karyotype that is associated with single copy losses of chromosomes 1, 2, 6, 10, 13, and 17. Notably, all derivative chromosomes were present in duplicate and no wild-type, unaltered versions of chromosomes 18 or 22 were observed. This suggests a history of chromosome loss followed by an event resulting in chromosome duplication that is consistent with previous reports of the chromosomal pattern in sarcomatoid ChRCC. (B) Short tandem repeat (STR) analysis of the patient's blood demonstrated varied, informative signals for 11 out of 15 of the highly variable repeat regions. The UOK276 cell line demonstrated loss of heterozygosity in 10 out of 11 informative variable repeat regions without loss of chromosomal number. The SKY analysis

of UOK276 showed retention of both the wild-type and derivative chromosomes and the STR marker on chromosome 8 was the only one to show two signal in both the cell line and the patient's blood. This loss of variation is also consistent with a history of chromosome loss followed chromosome duplication of the remaining single chromosome.

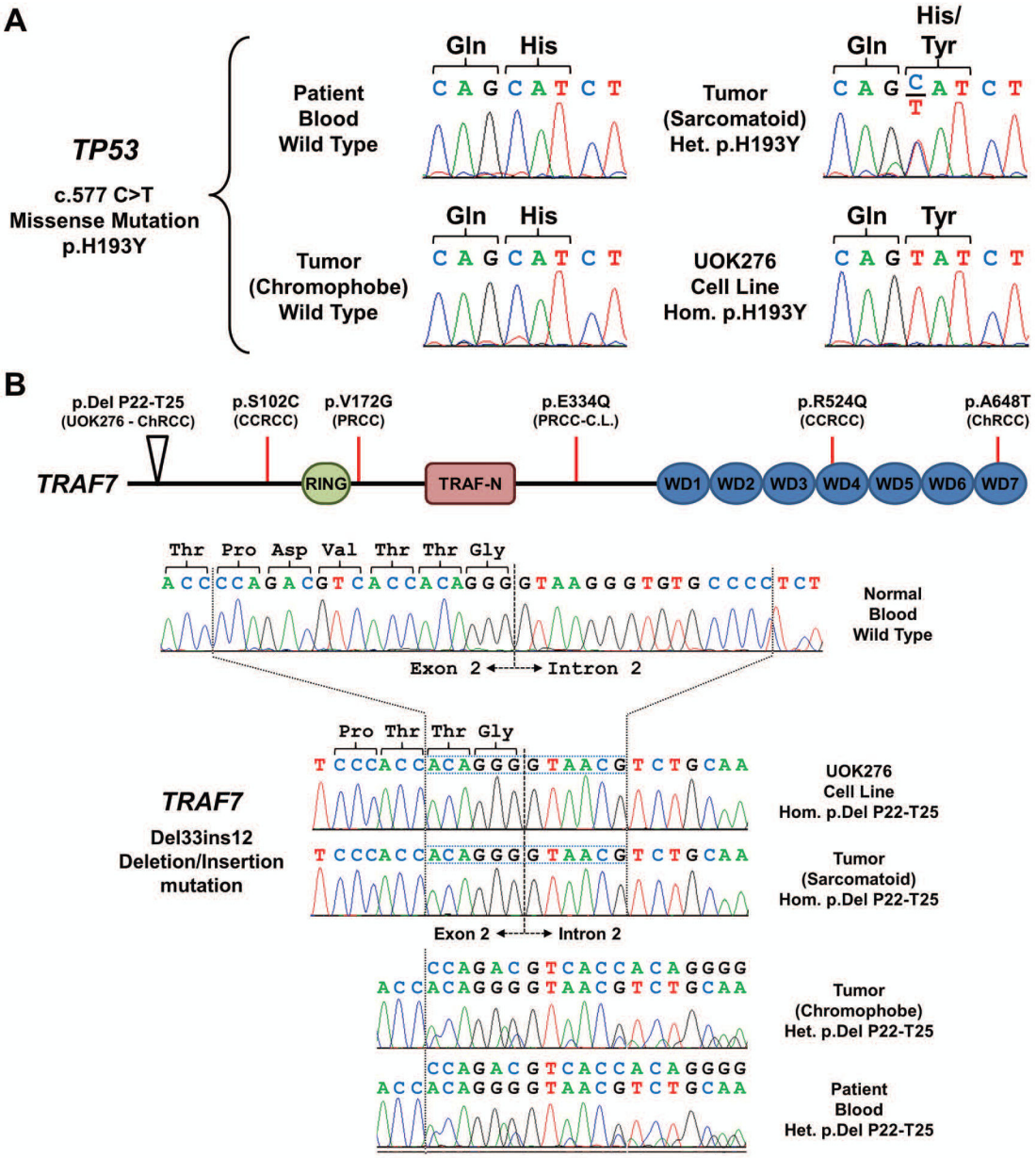

FIGURE 4.

Mutational analysis of the UOK276 cell line. (A) Mutation analysis identified a heterozygous missense mutation of *TP53* (c.577 C>T, p.H193Y) in the sarcomatoid region of the tumor that was not present in the chromophobe region of the tumor nor the germline DNA of the patient. This mutation was homozygous in the UOK276 cell line. (B) Mutation analysis identified a deletion/insertion mutation of *TRAF7* that removed 33 bp containing the end of exon 2 and the beginning of intron 2 and replaced 12 bp, resulting in the loss of 4 amino acids and retention of the last two amino acids of the exon and the canonical splice site. This mutation was present heterozygously in the germline DNA of the patient and in the chromophobe region of the tumor, but demonstrated loss of heterozygosity in the sarcomatoid region of the tumor and in UOK276. Somatic mutation within this gene have

been reported in several different kidney cancer types and these are mapped to the functional domains of TRAF and, although no mutations have been observed in the RING finger and TRAF N-terminal domains, mutation of one of the tryptophan-aspartic acid repeat (WD) domains has been reported. ChRCC, chromophobe RCC; CCRCC, clear cell RCC; PRCC, papillary RCC; C.L., cell line.

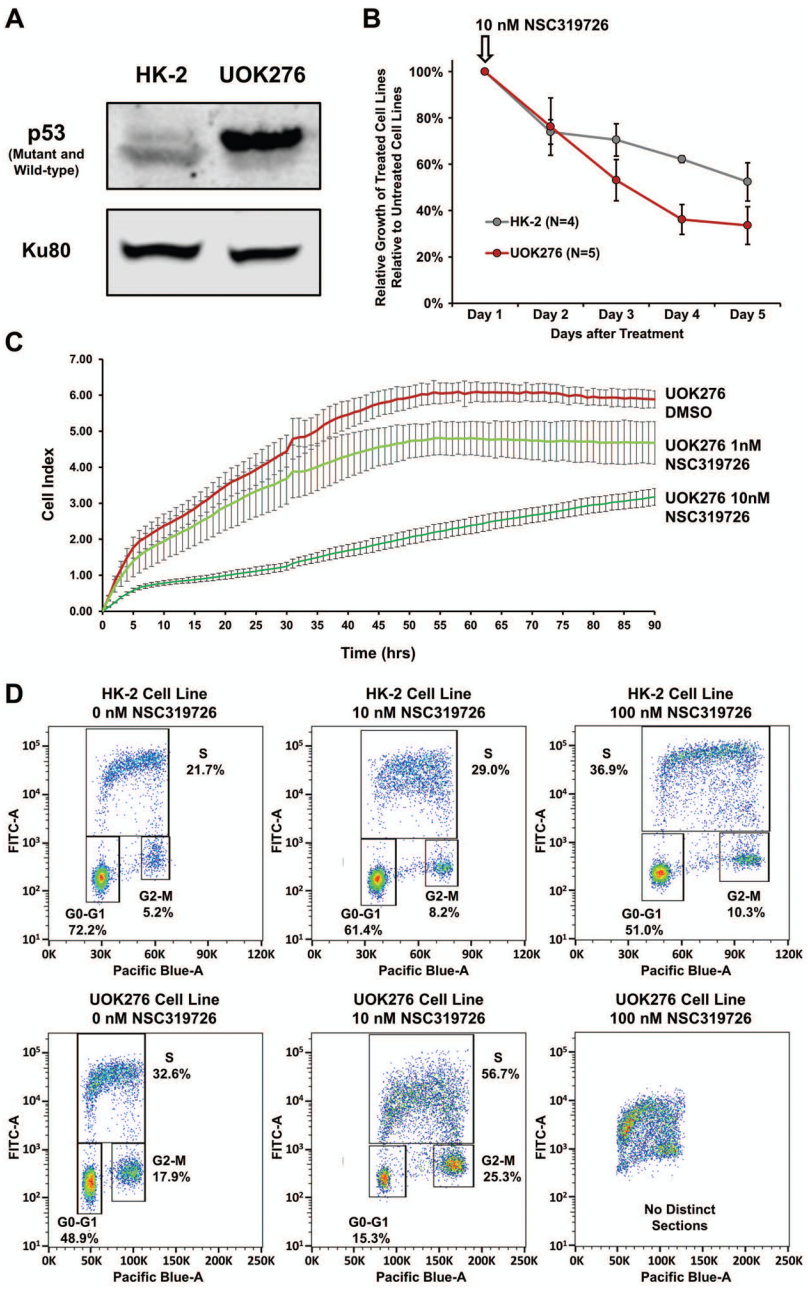

FIGURE 5.

TP53 Mutation Targeted Therapy. (A) Western blot analysis demonstrated that the mutant TP53 protein was expressed within the UOK276 cells, but not the HK-2 cells that were immortalized using a recombinant retrovirus containing the human papilloma virus (HPV 16) E6/E7 genes that promote TP53 protein degradation. (B) The effect of a single dose of the mutant TP53 reactivating drug 10 nM NSC319726 on cellular growth was evaluated for both the UOK276 and HK-2 cells and the relative number of cells between the treated and untreated cells was measured each day for 5 days using MTT assay. NSC319726 had a greater effect on the UOK276 cells than the HK-2 cells. This was repeated 3 times with 3

replicates in each experiment and the error bars represent standard deviation. (C) Real-time cell invasion assay analysis demonstrated a dose dependent suppression of invasion of UOK276 cells in response to a single starting dose of either 1 nM or 10 nM NSC319726 over a 90 h time period. Each time point represents the average of 4 replicates and the error bars represent standard deviation. (D) Bivariate cell cycle analysis, using BrdU to measure DNA synthesis and FxCycle Violet to measure DNA content, demonstrated that the increasing levels of NSC319726 had a greater effect on the cell cycle in the UOK276 cells in comparison to the HK-2 cells. The lower 10 nM dose produced a rapid decline in the percentage of UOK276 cells in G0/G1 and the higher 100 nM dose resulted in a complete loss of definable cell cycle phases.